To be submitted to ApJ

Numerical Model for Cosmic Rays Species Production and Propagation in the Galaxy

Ashraf Farahat, Ming Zhang and Hamid Rassoul

Department of Physics and Space Sciences, Florida Institute of Technology, Melbourne, FL 32901

and

J. J. Connell

Department of Physics and the Space Science Center, University of New Hampshire, Durham, NH 03824

ABSTRACT

In recent years, considerable progress has been made in studying the propagation and origin of cosmic rays, as new and more accurate data have become available. Many models have been developed to study cosmic ray interactions and propagation showed flexibility in resembling various astrophysical conditions and good agreement with observational data. However, some astrophysical problems cannot be addressed using these models, such as the stochastic nature of the cosmic rays source, small-scale structures and inhomogeneities in the interstellar gas that can affect radioactive secondary abundance in cosmic rays. We have developed a new model and a corresponding computer code that can address some of these limitations. The model depends on the expansion of the backward stochastic solution of the general diffusion transport equation (Zhang 1999) starting from an observer position to solve a group of diffusion transport equations each of which represents a particular element or isotope of cosmic ray nuclei. In this paper we are focusing on key abundace ratios such as B/C, sub-Fe/Fe, ^{10}Be/^{9}Be, ^{26}Al/^{27}Al, ^{36}Cl/^{37}Cl and ^{54}Mn/^{55}Mn, which all have well established cross sections, to evaluate our model. The effect of inhomogeneousity in the interstellar medium is investigated. The contribution of certain cosmic ray nuclei to the production of other nuclei is addressed. The contribution of various galactic locations to the production of cosmic ray nuclei observed at solar system is also investigated.

Subject headings: ISM: abundance — bubbles — cosmic rays

1. Introduction

The analysis of elemental and isotopic composition of cosmic ray nuclei that reach the solar system provides important information about their propagation and sources throughout the interstellar medium. Numerous numerical models have been developed for studying reacceleration, galactic halo size, antiprotons and positrons in cosmic rays, the interpretation of diffuse continuum gamma rays and even dark matter. The elemental and isotopic abundances ratio calculated using these techniques showed good agreement with observational data.

Many aspects, however, cannot be addressed using these models, e.g. the stochastic nature of the cosmic ray sources in space and time, which is important for high-energy electrons, and local inhomogeneities in the gas density that can affect radioactive secondary ratios in cosmic rays. Previous approaches to the nucleon propagation problem introduced by (Jones 1979) and (Bloemen et al. 1993) showed that energy losses are difficult to treat. Reacceleration was not considered in some of these approaches. These limitations motivated the need to develop a method that can handle some of these aspects. In this work we are introducing a numerical model that allows the study of cosmic rays production and propagation in the Galaxy. Using the backward stochastic solution of the general diffusion transport equation starting from an observer's position described by (Zhang 1999), we can calculate the elemental or isotopic abundance for a single cosmic ray nuclei. The same technique is applied to calculate the abundances for a certain number of nuclei by solving a group of diffusion transport equations, each represent a single nucleus.

In our study we used realistic astrophysical parameters like the gas density distribution, total and partial nuclei cross-sections. The code associated with this model is written in C++. Our code is sufficiently general such that we can include other physical effects such as energy losses and the effects of the local environment, e.g. the effect of the Local Supper Bubble surrounding the solar system and the giant clouds. The objective is to generate a model that can be improved with new astrophysical inputs and additional observational data, reflects realistic astrophysical conditions in the galaxy and finds justification for popular models of cosmic ray propagation. In this work we will focus on the calculation of B/C, sub-Fe/Fe, ^{10}Be/^{9}Be, ^{26}Al/^{27}Al, ^{36}Cl/^{37}Cl and ^{54}Mn/^{55}Mn ratios for evaluating our model. Most of these ratios have well established cross sections and accurate observational data over a wide energy range. The effect of the low density Local Super Bubble on the elemental and isotopic ratios observed at the interplanetary space is investigated. Using this model we can also investigate the contribution of some cosmic rays nuclides to the production of other nuclides and the contribution of different locations in the galaxy to the cosmic rays nuclei production.

2. Stochastic Solution to the Diffusion Equation

The general diffusion transport equation for the cosmic rays density distribution function $N_i(t,q)$ has the form (Berezinskiĭ et al. 1990)

$$\frac{\partial N_i}{\partial t} = f(\vec{\mathbf{r}},p) + \bigtriangledown \cdot (k_{\mathbf{xx}} \bigtriangledown N_i) - \vec{\mathbf{v}} \cdot \bigtriangledown N_i + \frac{\partial}{\partial p}\left[\left(b_i - \frac{p}{3}(\bigtriangledown \cdot \vec{\mathbf{V}})\right) N_i\right]$$
$$+k_{pp}\frac{\partial^2 N_i}{\partial p^2} - \frac{1}{p^2}\frac{\partial}{\partial p}(k_{pp}p^2)N_i - nv\sigma_i N_i - \frac{1}{\tau_i}N_i + \sum_{j<i} nv\sigma_{ij}N_j + \sum \frac{1}{\tau_{ij}}N_j. \quad (1)$$

Here $f(\vec{\mathbf{r}},p)$ is the source term; $k_{\mathbf{xx}}$ is the spatial diffusion coefficent; $b_i(\vec{\mathbf{r}},p)$ characterizes momentum (energy) loss rate dp/dt; V is the convection velocity; $P(\bigtriangledown \cdot V)/3$ describes the adiabatic momentum (energy) losses; $\sigma_i(p)$ is the inelastic scattering cross section of a nucleus of type i with nuclei of the interstellar gas; $n(\vec{\mathbf{r}})$ is the density of the interstellar gas; v is the velocity of the nucleus; σ_{ij} is the production cross section for a nuclei of type j from heavier nuclei of type i where $j < i$; τ_i is the life time of a nucleus of type i with respect to radioactive decay; τ_{ij} is the mean lifetime for the production of species j as a daughter nucleus in the radioactive decay of species i. In case of including reacceleration, the momentum-space diffusion coefficient k_{pp} is calculated using the formula suggested by (Seo & Ptuskin 1994) and (Berezinskiĭ et al. 1990) where

$$k_{pp} = \frac{4p^2{v_A}^2}{3\delta(4-\delta^2)(4-\delta)\xi}\left(\frac{1}{k_{\mathbf{xx}}}\right)$$

where the ratio of wave energy density to magnetic field energy density $\xi = 1$, v_A is the Alfvén speed and the constant $\delta = 0.36$.

The spatial position and momentum of a particle in diffusion process, obeys the following set of stochastic differential equations (Zhang 1999):

$$d\vec{\mathbf{X}}_s^{t,\vec{\mathbf{x}}} = \sqrt{2k_{\mathbf{xx}}}d\vec{W}_{\mathbf{x}}(s) + \vec{\mathbf{V}}ds, \vec{\mathbf{X}}_0^{t,\vec{\mathbf{x}}} = \vec{\mathbf{x}} \in D \quad (2)$$

$$dP_s^{t,\vec{\mathbf{x}}} = \sqrt{2k_{pp}}dW_p(s) + \left[-b - \frac{1}{3}(\bigtriangledown \cdot \vec{\mathbf{V}})P\right]ds, s \geq 0. \quad (3)$$

where D is a bounded domain, $W_{\mathbf{x}}(t), W_p(t)$ are four dimensional Wiener processes having independent increments and continuous trajectories, and for which $EW_i(t) = 0$ (E being the

mathematical expectation sign). The parameters $K_{\mathbf{xx}}$, K_{pp}, b normally depend on particles species, however if P is given in momentum per nucleon, the parameters $k_{\mathbf{xx}}$, k_{pp}, b are assumed to be no longer species dependent. When many particles are simulated, average behavior of the diffusion process can be investigated. The stochastic process starts from q at time t ($s = 0$) and it steps back in time as the integration variable s increases until $s = T$ or time 0.

The diffusion equation (1) can be written in the form

$$LN = f(\vec{\mathbf{r}}, p) - cN \tag{4}$$

where

$$L = \frac{1}{2}\sum_{i,j}\alpha^{i,j}(t,\mathbf{q})\frac{\partial^2}{\partial\mathbf{q}^i\partial\mathbf{q}^j} + \sum_i \beta^i(t,\mathbf{q})\frac{\partial}{\partial\mathbf{q}^i} - \frac{\partial}{\partial t}$$

where the $\mathbf{q}^i\{i = 1,..,4\} = \{\mathbf{x}, p\}$ is composed of particle position and momentum, $\alpha^{i,j}$ represents a non-negative and symmetric diffusion coefficient tensor, $\beta^i(t,q)$ represents the drift term.

Equation (4) has a stochastic solution in the form (see Appendix A):

$$N(t,\mathbf{q}) = E\int_0^T f(\mathbf{Q}_t^{t,\mathbf{q}})exp\left(-\int_0^t c(\mathbf{Q}_s^{t,\mathbf{q}})ds\right)dt \tag{5}$$

where $\mathbf{Q} = \{\vec{\mathbf{x}}, p\}$ is 4-d stochastic process, $E[Y]$ is defined as the expectation value of a random variable or a function of random variables $[Y]$ with respect to the distribution space of all stochastic processes, T is the time needed for the stochastic process to run backward from q at time t till it gets to the boundary ∂D. The stochastic solution in equation (5) describe the case where $N(t,\mathbf{q})$ is the number of particles that arrived in a location $\mathbf{q}$ at time t, such as the particles that arrive at the solar system. These particles come through various stochastic paths from locations in the galaxy at time 0. The notation $\mathbf{Q}_s^{t,\mathbf{q}}$, describes the path of the particles starting at time $t = 0$. The average number of particles arriving at the point $\mathbf{q}$ is estimated by averaging all possible stochastic path process for many test particles starting at different locations and ended up at the location $\mathbf{q}$. The exponential term contains the integration of $c(t,\mathbf{q})$ along the stochastic path allows the stochastic process to be destroyed at an exponential rate as a function of time. The parameter $c(t,\mathbf{q})$ contains terms describing the inelastic and production cross sections; density and mean life time.

Figure 1 shows a graphical representation for the simulation as a number of different stochastic processes described by equation (2) or (3) run backward in time from $s = 0$ to

$s = t$, all starting from the same location $\mathbf{q}$ at time t until hitting some position $\mathbf{q_0}$. Each of these paths should be weighted with the exponential factor $exp\{-\int_0^t c(\mathbf{Q}_s^{t,\mathbf{q}})ds\}$. In other words the average number of particles arriving at the location $\mathbf{q}$ is the average value at the end of the backward stochastic process weighted by the exponential factor.

Equation (5) can be applied to determine the cosmic ray density distribution for any nuclei. In this work we consider 87 nuclei starting from ^{64}Ni to ^{1}H.

In case of ^{64}Ni equation (5) takes the form:

$$N_{(^{64}Ni)}(t,\mathbf{q}) = E\int_0^T f(\mathbf{Q}_t^{t,\mathbf{q}})exp\left[-\int_0^t \left(nv\sigma_{(^{64}Ni)} + \frac{1}{\tau_{(^{64}Ni)}}\right)ds\right]dt \tag{6}$$

and in case of ^{62}Ni we get the form:

$$N_{(^{62}Ni)}(t,\mathbf{q}) = E\int_0^T \left[f(\mathbf{Q}_t^{t,\mathbf{q}}) + nv\sigma_{(^{64}Ni\rightarrow{}^{62}Ni)}N_{(^{64}Ni)} + \frac{1}{\tau_{(^{64}Ni\rightarrow{}^{62}Ni)}}N_{(^{64}Ni)}\right] exp\left[-\int_0^t (nv\sigma_{(^{62}Ni)} + \frac{1}{\tau_{(^{62}Ni)}}ds\right]dt \tag{7}$$

The first three terms in the right side of equation (7) represent the source of ^{62}Ni including that produced from the spallation of ^{64}Ni, however these spallation terms do not appear in equation (6) because we assume that ^{64}Ni is the heaviest element under consideration.

The same procedure can be repeated down to ^{1}H such that the c term will describe all possible transformation from heavier nuclei to the nucleus under consideration.

3. Model Description

The above described backward stochastic technique can be applied to calculate the elemental and isotopic abundances of the cosmic ray nuclei reaching the solar system. Cosmic ray nuclei observed in the solar system are produced at different locations in the galaxy and propagate through different stochastic paths until reaching the solar system. Elemental abundance in the solar system are calculated by allowing test particles to start at time $s = 0$ at the solar system location and propagate backward in time till reaching the galaxy boundary. The average abundance of a certain cosmic rays nucleus can be estimated by simulating many particles trajectories and weighting the average with the exponential function.

Nuclei cross sections and their decay life times play a major role in the elemental and isotopic abundances observed at the solar system. Cosmic ray nuclei observed in the solar system are produced as a result of interactions and decays of the primary cosmic ray nuclei produced at their sources. All of these interactions have to be taken into consideration in order to predict the correct abundances.

(Strong & Moskalenko 1998) introduced a technique to predict the cosmic ray abundances at the solar system by solving a reaction network starting at the heaviest nuclei (i.e. ^{64}Ni), solving the propagation equation, computing all the resulting secondary source functions, and proceeding to the nuclei with A - 1. The procedure is repeated down to A = 1. In this way all secondary, tertiary etc. reactions are automatically included. Their method showed satisfactory agreement with the observational data; however it is not possible to describe the effect of small scale structure in the galaxy using this technique.

Solving individual diffusion equations for each element is a long and inefficient processes. In this work we describe a new method that enables the solution of only one diffusion equation that describes all nuclei under consideration. In this case equation (1) is written in the form

$$\frac{\partial N}{\partial t} = F + \bigtriangledown \cdot (k_{\mathbf{xx}} \bigtriangledown N) - \vec{\mathbf{v}} \cdot \bigtriangledown N + \frac{\partial}{\partial p}\left[\left(b - \frac{p}{3}(\bigtriangledown \cdot \vec{\mathbf{V}})\right) N\right] + k_{pp}\frac{\partial^2 N}{\partial p^2} - \frac{1}{p^2}\frac{\partial}{\partial p}(k_{pp}p^2)N - CN \tag{8}$$

where

$$N = \begin{pmatrix} ^{64}Ni_c \\ ^{62}Ni_c \\ ^{60}Ni_c \\ .. \\ .. \\ ^{1}H_c \end{pmatrix}, \quad F = \begin{pmatrix} ^{64}Ni_s \\ ^{62}Ni_s \\ ^{60}Ni_s \\ .. \\ .. \\ ^{1}H_s \end{pmatrix} * f(\vec{\mathbf{r}}, p),$$

where the vector N represents the calculated abundances at the solar system, F represents the source abundances and $f(\vec{\mathbf{r}}, p)$ is the source distribution function given as in Table 1. The composition of the source is assumed to be uniform.

The 1 -d $c(\mathbf{Q}_s^{t,\mathbf{q}})$ term in equation (5) is replaced by the $((M \times M), M = 87)$ C matrix in the multidimensional solution where M is the number of nuclei under investigation

$$C = \begin{pmatrix} c_{11} & 0 & 0 & .. & 0 \\ c_{21} & c_{22} & 0 & .. & 0 \\ .. & .. & .. & .. & .. \\ .. & .. & .. & .. & .. \\ c_{M1} & c_{M1} & .. & .. & c_{MM} \end{pmatrix},$$

where the components c are defined as

$$c_{ii} = nv\sigma_i + \frac{1}{\tau_i}$$
$$c_{ij} = -nv\sigma_{ij} - \frac{1}{\tau_{ij}}$$

In equation (8) we extended equation (1) in a matrix format such that it represents 87 elements instead of one element. Terms in this equation contain all factors participating in the production and the decay of a certain cosmic ray nucleus. For example the matrix row that describes ^{10}Be should contain the total inelastic cross section of this element and its decay life time (destroying terms) and the production cross sections from all other elements that are possibly participating in the production of ^{10}Be and the mean life time of the production of ^{10}Be from these elements (production terms). We are assuming same energy dependent diffusion coefficient for all participating nuclei and same energy loss rates. The model has some limitations as it uses the same diffusion coefficient in all transport equations and also the same energy losses have to be used for all the elements. The average interstellar medium density was taken as in Moskalenko et al. (2002). The solution of equation (8) is given as:

$$N = E \int_0^T exp\left[-\int_0^t C ds\right] F(t) dt \tag{9}$$

Each of the C diagonal elements represents a loss of a certain nuclei either by spallation and / or decay as each of these diagonal elements stands for the multiplication of [(average ISM density × velocity of the cosmic rays nucleus × inelastic cross section of the nucleus) + (life time of that nucleus)], on the other hand, the off diagonal elements describe the production of the cosmic rays nuclei and each term represents the multiplication of [-(average ISM density × velocity of the cosmic rays nucleus × production cross section of the nucleus) − (mean life time for the production of the nucleus from other nuclei)]. The simulation includes a few thousand stochastic trajectories and the average abundance for each element at the solar system is estimated. We allow free escape at galactic radius R_h and the halo size $\pm z_h$. We take $R_h = 30$ kpc and $z_h = 4$ kpc. The He/H ratio is 0.11 by number and

$d\mathbf{V}/dz = 0$. Isotopic cross sections are calculated using (Webber et al. 1990; Sihver et al. 1993). The solar modulation numerical model ("SolMod" Fisk (1971)) is used to modulate interstellar medium spectrum.

4. Model Verification

We mainly investigated the B/C ratio for testing our model as it is one of the most accurately measured ratios covering a wide energy range and having well established cross sections.

Figure 2 shows the calculated B/C ratio in local interstellar space (LIS) (solid curve) and 500 MV modulated (dashed curve) B/C ratio compared with the observational data from HEAO-3 (Webber et al. 1996), ACE (Davis et al. 2000) and Ulysses (DuVernois et al. 1996). Model parameters are shown in Table 1. k_0, δ, ρ_0, and z_h and dV/dz are chosen to best fit the observational data and to produce the characteristic shape of the measured B/C ratio. Since the inclusion of the convection effects is not sufficient to fit the data even at low modulation level, we have to use a model with a break in the spatial diffusion coefficient $k_{\mathbf{xx}}$ at $\rho_0 = 3$ GV. The value of $\delta = 0.36$ gives the best match, while other values gives less satisfactory agreement with the data where

$$\delta = \begin{cases} 0.36 & \text{if } \rho > \rho_0; \\ -0.36 & \text{if } \rho < \rho_0. \end{cases}$$

The model reproduces the peak very well and fit the data for energies above 1 GeV/nucleon as the effect of the solar modulation is negligible for high energy ranges. The modulation parameter is used to describe the modulation level. However the modulation effects produced by different modulation models using the same modulation parameter are slightly different. The uncertainty due to the variation in the halo size is only about 10% (Strong & Moskalenko 2001). A halo size of 4 kpc shows satisfactory agreement with the data. High energy B/C ratio shows little disagreement with HEAO-3 data and this is because we use a single power-law injection index.

In Figure 3 we calculate the (LIS) (solid curve) and 500 MV modulated (dashed curve) for the second key cosmic rays ratio (Sc+Ti+V)/Fe compared with observations from HEAO-3 (Binns et al. 1988), ACE (Davis et al. 2000) and Sanriku experiment (Hareyama 1999). The ratio shows the best consistentcy with observations because the sub-iron elements are mainly produced from iron.

Figure 4 shows ^{10}Be/^{9}Be (LIS) (solid curve) and 450 MV modulated (dashed curve).

The model did not show a satisfactory agreement compared to the observational data from ISOMAX, ISEE3 and IMP7 and 8 and shows better agreement with Voyager (Lukasiak et al. 1999) and Ulysses (Connell 1998) observations. Large uncertainty ~15% in the production cross sections of ^{10}Be will produce this disparity. An over prediction of ^{9}Be compared to the measurements (Connell 1998) and (Lukasiak et al. 1999) is another potential reason for data contradictory. Modifying the source abundance will not change the ^{10}Be/^{9}Be ratio since both products are mainly secondaries. Uneven diffusion coefficient across the halo will also help in better data fitting but will not completely solve the fitting problem. Figures 5 - 7 show the heavier radioactive nuclei ^{26}Al/^{27}Al, ^{36}Cl/^{37}Cl and ^{54}Mn/^{55}Mn. A scale height of $z_h = 4$ kpc and $d\mathbf{V}/dz = 0$ was applied in all the above calculations.

5. Results

5.1. Effect of the Local Supper Bubble

The effect of the inhomogeneities in the interstellar medium can be described using this model. Figure 8 shows the effect of the low-density 0.06 particles/cm^3 and an average radius of 200 pc region, which simulates the Local Super Bubble surrounding the solar system on the production of the ^{10}Be/^{9}Be. The ratio apparently decreased at lower energies due to the decay of the radioactive ^{10}Be with lifetime of 3.1 million years which decrease its diffusion distance and make the effect of the Bubble significant; however the effect of the low-density region will be negligible at very high energies due to the relativistic lifetime of the nuclei at these energies. The existence of the bubble was found to have a minimal effect on the abundance ratio of stable nuclei while having significant effects on radioactive nuclei (Farahat et al. 2003) because the half life limits the distance of the radioactive elements source. The Source/Solar system abundances have been taken from (Anders et al. 1989), however the source abundance error can be as large as 100% (Strong & Moskalenko 2001).

5.2. Elemental Contribution

Cosmic ray elements and isotopes observed at the solar system are either primary or produced due to interaction of primary and secondary nuclide with the interstellar medium or due to the decay of radioactive nuclide. The contribution of a heavy nuclide to the production of lighter ones is mainly dependent on the production cross sections, however these cross sections are different from one interaction to the other which results in an unequal participation of the nuclide to the production of other elements or isotope.

Using the new propagation model we can determine which nuclides make the most contribution to the production of other element or isotope at certain energies. In the simple case and by using equation (5) we can calculate the contribution of any element to the production of another element by knowing the production cross section and the source distribution. The solution can be expanded, as mentioned previously, in the form of equation (9) where we can calculate the abundance of any element due to the contribution of other nuclide. In this case each component in the lower triangular matrix is describing the contribution of one nuclide to the production of another element or isotope.

Carbon is mainly contributing to the production of Boron $\sim$ 55% as shown in figure 9, Oxygen is contributing by $\sim$ 30%, and the rest $\sim$ 15% from the participation of other nuclei. The partial production cross-section of the B from C is high when compared to the production from other elements. Carbon has a fairly high source abundance which makes it one of the major primary nuclei participating in the production of secondary Boron components observed at the solar system.

Figure 10 shows that about $\sim$ 45% of the produced Beryllium is produced by Carbon contribution while $\sim$ 30% is produced by Oxygen contribution; the remaining $\sim$ 25% are mainly produced by the contribution of Iron, Magnesium, Neon, Silicon and others. Most of the observed Carbon is primary; other contributions are mainly due to the interaction of Oxygen nuclei with the interstellar medium as shown in figure 11.

In Figure 12 we show that Iron is the main contributor $\sim$ 90% to the Chlorine production. Figure 13 shows that the main three elements contributing to the production of Neon are the Neon, Magnesium $\sim$ 30% and Silicon $\sim$ 28%. From Figures 9 - 13 we conclude that cosmic rays nuclei are mainly created due to a major contribution of only few cosmic rays nuclei and minor or zero contribution of others. This result can lead to simplify numerical models used to calculate the elemental and isotopic abundance of cosmic rays by only including elements that really contribute to the production of a certain nuclei. Using these results we are able to track the primary cosmic rays nuclei to determine what percentage will contribute to the production of other nuclei and what will remain without contribution to other members and arrive to the interplanetary space. Production cross sections and the source abundances are the main two factors determining the production contribution for each nucleus. The local density of the interstellar space is also considered as an important factor to determine the production of elements since the propagated nuclei pass through low and high density regions. The results in figures 9 - 13 were calculated at 1 GeV/nucleon.

5.3. Location Contribution

Different locations in the galaxy are unequally participating into the production of elements and isotopes observed in the solar system. Using the new method introduced in this paper we can determine the locations in galaxy containing the sources of the production of a certain nuclide, this means if ^{12}C, ^{56}Fe, ..etc participate in the production of ^{10}B observed at the solar system we determine the locations at which ^{12}C, ^{56}Fe, ..etc were produced. A test particle is allowed to follow a stochastic path starting from the solar system at time t and runs backward in time till hitting the galaxy boundary. The abundance for each nucleus is recorded at certain energy and a single location in the stochastic path. The smaller the time step the more detailed information can be obtained from the locations contribution however, computational time is inversely proportional to the time step. We divide the galaxy into a set of squares each 40×40 pc and the sum of all abundances.

The upper plots of figures 14 - 17 show an image plot for different locations contributing to the production of the sources of ^{10}B, ^{10}Be, ^{20}Ne and ^{12}C respectively normalized to carbon = 100 and the lower plots show the abundance at Y = 0 kpc and X runs from -20 to 20 kpc. Due to the decay of ^{10}Be the curve is more peaked than the stable Boron curve. The results in figures 14 - 17 were calculated at 1 GeV/nucleon

We investigated several locations contribution within certain region surrounding the solar system. The model shows that most of the cosmic rays observed in the solar system are from sources within 10 kpc around the solar system. The very low abundance regions appear in the ^{10}B and ^{10}Be distributions near the center of the galaxy is due to the interstellar medium density distribution (Moskalenko et al. 2002) with lower number density around the galactic center which will be reflected on the number of interactions with the interstellar medium producing ^{10}Be and ^{10}B.

6. Conclusion

We introduced a new numerical model to calculate the elemental and isotopic abundances of cosmic rays. The model depends on solving a group of diffusion transport equations each representing a particular element or isotope using the backward Markov Stochastic technique staring at an observer location in the solar system and stoping at the galaxy boundaries. Diffusion coefficient, halo size and rigidity are the main parameters contributing to this model and are chosen to best fit the observational data. Primary to secondary ratio have been used to validate the model. The results show good agreement with the B/C ratio which have the best determined cross sections over a wide energy range. SubFe/Fe fits the

data very well. The model show less satisfactory agreement in the case of $^{10}Be/^{9}Be$ due to the over estimated source abundance of ^{9}Be and poorly determined cross sections. The uncertainty in estimating the cross sections ranged from 20% - 35%. The effect of the inhomogeneities in the interstellar space is investigated as the model allows us to address small scale structure inside the galaxy in our calculations. The solar system is embedded in a very low density region with a radius of 200 pc called the Local Super Bubble. The existence of the Bubble affects the abundances of the short lived isotopes as the size of the Bubble is significantly compared to their diffusion length. $^{10}Be/^{9}Be$ abundance ratio is reduced by taking the low density Bubble region into consideration. The low density region also results in less interaction of the cosmic ray nuclei with the interstellar space which will clearly affect the observed solar system elemental abundance. The model can describe not only the elemental and isotopic abundances variation at the solar system but anywhere in the Galaxy. The model shows that nuclei observed in the interplanetary space are produced due to an uneven contribution of the elements in the galaxy. In this model, the source contribution to a particular cosmic ray species observed at the solar system can be calculated. Carbon was found as a dominant contributor to the production of ^{10}B and ^{10}Be due to its large production cross section. Elemental percent contribution to various cosmic rays nuclei investigated using this model. Carbon and Oxygen found to be the main source for Boron production. About $\sim$ 45% of the produced Beryllium come from Carbon. The production of Carbon is mainly related to the interaction of Oxygen nuclei with the interstellar medium. Iron is the main element contributing to the Chlorine production and $\sim$ 42% are primary Carbon. Neon is produced from the interactions of Magnesium, Silicon and small iron percentage Iron. The model shows flexibility not only in determination of the elements contribution but also to find the locations which mainly contributing to the production of a certain element. The contribution of different locations in the galaxy to the production of ^{10}B, ^{10}Be, ^{20}Ne and ^{12}C and was investigated. Different diffusion coefficients and different energy losses in the diffusion equations describing various nuclei can't be handled using this model. The major uncertainty in our calculations resulted from the cross-sections and modulation errors. Observations at higher energies are greatly helpful in reducing the uncertainty in modulation.

We are grateful to A. W. Strong, I. W. Moskalenko for providing cross sections used in this work and for helpful discussions. We thank B. Ball for useful suggestions. The work is supported in part by NASA under grants NAG5-10888 and NAG5-11036 and the Egyptian government grant GM477. For any questions contact ashraf@pss.fit.edu.

A. Applications to the Ito Formula

The general diffusion equation takes the form

$$Lu(t,\mathbf{q}) + c(t,\mathbf{q})u(t,\mathbf{q}) = f(t,\mathbf{q}), \quad \mathbf{q} \in D \tag{A1}$$

where D is a bounded domain with a smooth boundary ∂D, functions $c(t,\mathbf{q})$, $f(t,\mathbf{q})$ are assumed bounded and continuous.

The second-order differential operator is defined as

$$L = \frac{1}{2}\sum_{i,j}\alpha^{i,j}(t,\mathbf{q})\frac{\partial^2}{\partial\mathbf{q}^i\partial\mathbf{q}^j} + \sum_i \beta^i(t,\mathbf{q})\frac{\partial}{\partial\mathbf{q}^i} - \frac{\partial}{\partial t} \tag{A2}$$

where α is the diffusion coefficent tensor, β is the drift term containing the components b^i

The Ito formula expresses the calculus of changing stochastic variables. Let the Ito formula to be applied on the function

$$u\left(t,\mathbf{Q}_t^{t,\mathbf{q}}\right) exp\left[-\int_0^t c\left(\mathbf{Q}_s^{t,\mathbf{q}}\right) ds\right].$$

where

$$d\mathbf{Q}_s^{t,\mathbf{q}} = \sum \sigma\left(\mathbf{Q}_s^{t,\mathbf{q}}\right) dW_s + \beta\left(\mathbf{Q}_s^{t,\mathbf{q}}\right) ds, \mathbf{Q}_0^{t,\mathbf{q}} = \mathbf{q}$$

and the vector σ is related to the diffusion coefficient tensor α by

$$\alpha^{i,j}(t,\mathbf{q}) = \sum \sigma^i(t,\mathbf{q})\sigma^j(t,\mathbf{q});$$

we get

$$\begin{aligned}
&u\left(t-t_2,\mathbf{Q}_{t_2}^{t,\mathbf{q}}\right) exp\left\{Y\left(\mathbf{Q}_{t_2}^{t,\mathbf{q}}\right)\right\} - u\left(t-t_1,\mathbf{Q}_{t_1}^{t,\mathbf{q}}\right) = \\
&\int_{t_1}^{t_2}\left[Lu\left(t-t_1,\mathbf{Q}_{t_1}^{t,\mathbf{q}}\right) - f\left(t-t_1,\mathbf{Q}_{t_1}^{t,\mathbf{q}}\right) + c\left(\mathbf{Q}_{t_1}^{t,\mathbf{q}}\right) u\left(t-t_1,\mathbf{Q}_{t_1}^{t,\mathbf{q}}\right)\right] exp\left\{Y\left(\mathbf{Q}_s^{t,\mathbf{q}}\right)\right\} dt \\
&+ \int_{t_1}^{t_2} f\left(t-t_1,\mathbf{Q}_{t_1}^{t,\mathbf{q}}\right) exp\left\{Y\left(\mathbf{Q}_s^{t,\mathbf{q}}\right)\right\} dt \\
&+ \int_{t_1}^{t_2} \nabla u\left(t-t_1,\mathbf{Q}_{t_1}^{t,\mathbf{q}}\right) exp\left\{Y\left(\mathbf{Q}_s^{t,\mathbf{q}}\right)\right\} \sigma\left(\mathbf{Q}_{t_1}^{t,\mathbf{q}}\right) dW_t
\end{aligned} \tag{A3}$$

Using equation (A1), the first integral on the right-hand side of equation (A3) becomes 0. Then, taking average of both sides of (A3), since $\langle dW\rangle = 0$, we get

$$\begin{aligned}
&E\left[u\left(t-t_2,\mathbf{Q}_{t_2}^{t,\mathbf{q}}\right) exp\left\{-\int_0^t\left(\mathbf{Q}_s^{t,\mathbf{q}}\right) ds\right\} - u\left(t-t_1,\mathbf{Q}_{t_1}^{t,\mathbf{q}}\right)\right] = \\
&\qquad E\left[\int_{t_1}^{t_2} f\left(t-t_1,\mathbf{Q}_{t_1}^{t,\mathbf{q}}\right) exp\left\{-\int_0^t c\left(\mathbf{Q}_s^{t,\mathbf{q}}\right) ds\right\} dt\right]
\end{aligned} \tag{A4}$$

Let $t_1 = 0$ and $t_2 = T$ the first exit time for the stochastic process get to the boundary ∂D. since, $\mathbf{Q}_0^{t,\mathbf{q}} = \mathbf{q}$, $E\left[u\left(t, \mathbf{Q}_0^{t,\mathbf{q}}\right)\right] = u\left(t, \mathbf{q}\right)$Therefore, from equation (A3) we get the solution for the general diffusion equation (A1) as

$$u\left(t, \mathbf{q}\right) = \int_0^T f\left(t, \mathbf{q}\right) exp\left\{-\int_0^t c\left(\mathbf{Q}_s^{t,\mathbf{q}}\right) ds\right\} dt \tag{A5}$$

For detailed proof of the above formula and more applications of stochastic differential equations see (Freidlin 1985; Gardiner 1983; Øksendal 1992)

B. Matrix Exponential

The exponential of a matrix could be calculated in many ways such as Padé approximation, differential equations, the matrix eigenvectors, series method, and the matrix characteristic polynomial. The method used is depending on the naive approach of finding eigenvalues D and eigenvectors V of the matrix A_{mn} such that

$$A_{mn} = VDV^{-1}, \tag{B1}$$

since V is nonsingular we have

$$exp(A_{mn}) = Ve^{D}V^{-1}. \tag{B2}$$

Matrix exponential calculation is very reliable and straightforward using this method, however theoretical difficulty occurs if there is no invertible matrix of eigenvectors V. For detailed description of methods that can be used to compute the exponential of a matrix and additional comparisons between these methods see (Moler & Loan 2003).

REFERENCES

Anders, E., & Grevesse, N. , 1989, Acta, 53, 197

Berezinskiĭ, V. S., et al., 1990, Astrophysics of Cosmic Rays (Amsterdam: North-Holland).

Binns, W. R., Garrard, T. L., Israel, M. D., et al., 1988, ApJ, 324, 1106.

Bloemen et al., 1993 , A&A, 267, 372B.

Connell, J. J., 1998, ApJ, 501, 59

Davis, A. J., Mewaldt, R. A., Binns, W. R., et al., 2000, AIP Conf. Proc., 528, 421.

DuVernois, M. A.,& Thayer, M. R., 1996, ApJ, 465, 982.

Farahat, A., Zhang, M. , Rassoul H., & Connell J. J. 2003, 28th ICRC (Tsukuba), 3, 1957

Fisk, L. A., 1971, J. Geophys. Res., 76, 221

Freidlin, M., 1985, Functional Integration and Partial Differential Equations (Princeton: Princeton Univ. Press)

Gardiner, C. W., 1983, Handbook of Stochastic Methods for Physics, Chemistry and the Natural Sciences (Berlin: Springer)

Hareyama, M., et al., 1999, 26th ICRC (Salt Lake City), 3, 105.

Jones, W. V., 1979, AIPC, 49, 41J

Lukasiak, A. F., McDonald, F. B., & Webber W. R., 1999, 26th ICRC (Salt Lake City), 3, 41

Moler, C. B. & Loan, C. V. 2003, SIAM Review, 45, 3

Moskalenko, I. V., Strong, A. W. , Ormes J. F., &Potgieter M. S. 2002, ApJ, 565, 280

Øksendal, B. K., 1992, Stochastic Differential Equations: An Introduction with Applications (New York: Springer)

Press et al., Numerical Recipes 2nd ed.; Cambridge: Cambridge Univ. Press)

Seo, E. S., & Ptuskin, V. S. 1994, ApJ, 431, 705

Sihver, L., Tsao, C. H. , Silberberg, R., Kanai, T. & Barghouty, A. F. 1993, Phys. Rev. C, 47, 1225

Strong, A. W., & Moskalenko, I. V. 2001, Adv. Space Res, 27, 717

Strong, A. W., & Moskalenko, I. V. 1998, ApJ, 509, 212

Webber, W. R., Lukasiak, A., McDonald F. B., & Ferrando, P. , 1996, ApJ, 457, 435

Webber, W. R., Lee, M. A., & Gupta, M. , 1992, ApJ, 390, 96

Webber, W. R., Kish, J. C., & Schrier, D. A., 1990, Phys. Rev. C, 41, 533W

Zhang, M., 1999, ApJ, 513, 409

Table 1. Model Parameters

Source Distribution	$f(\vec{\mathbf{r}}, p) = f_0 \left(\frac{R}{R_0}\right)^{0.5} exp\left(-\frac{R-R_0}{R_0} - \frac{\|z\|}{0.2kpc}\right)$ f_0 is a normalization constant
Spatial Diffusion Coefficient	$k_{xx} = \left(\frac{v}{c}\right) k_0 \left(\frac{\rho}{\rho_0}\right)^{\sigma}$, $k_0 = 6 \times 10^{28} cm^2/s, \quad \rho_0 = 3 \quad GV$
Injection Spectrum	$df/dp \propto p^{-2.35}$
Convection Velocity (z-direction)	$V = 20km/s$
Halo Height	$Z_h = 1 - 10kpc$
Galactic Radius	$R_h = 30kpc$
Distance from the Sun to the Galactic Center	$R_0 = 8.5kpc$

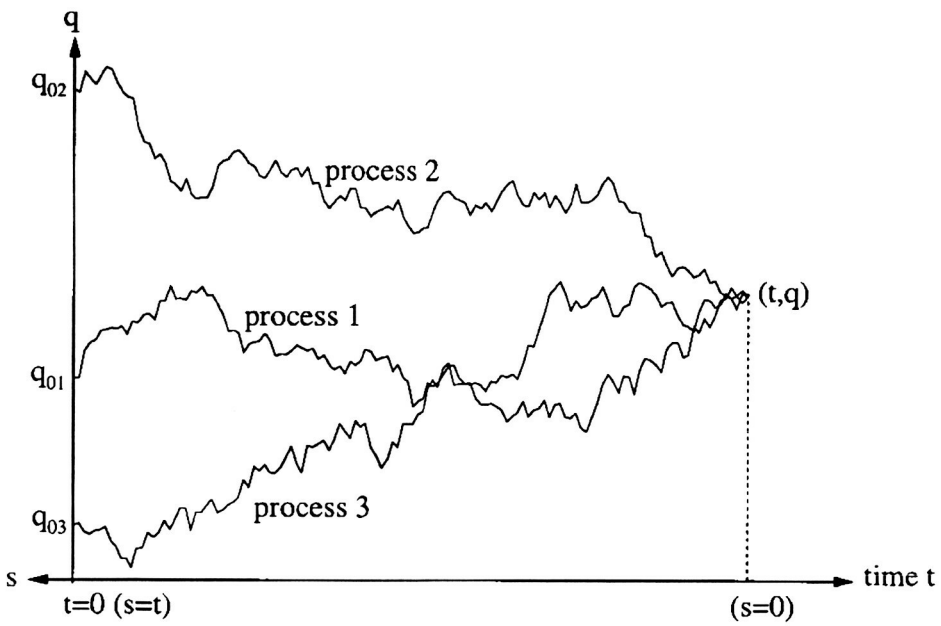

Fig. 1.— Graphical illustration of using backward stochastic processes to obtain the solution to general diffusion equations.

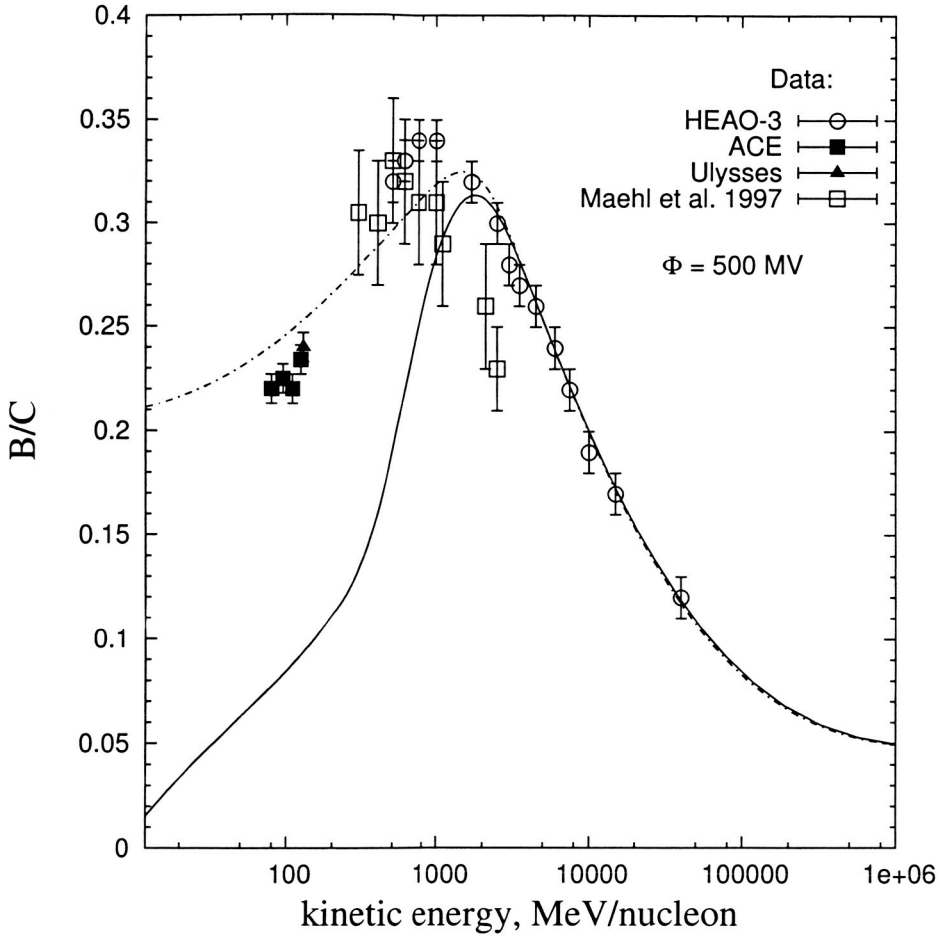

Fig. 2.— B/C ratio calculated for $z_h = 4$ kpc and $dV/dz = 0$. Solid curve (lower) local interstellar medium, dashed-dotted curve (upper) modulated $\phi = 500$ MV.

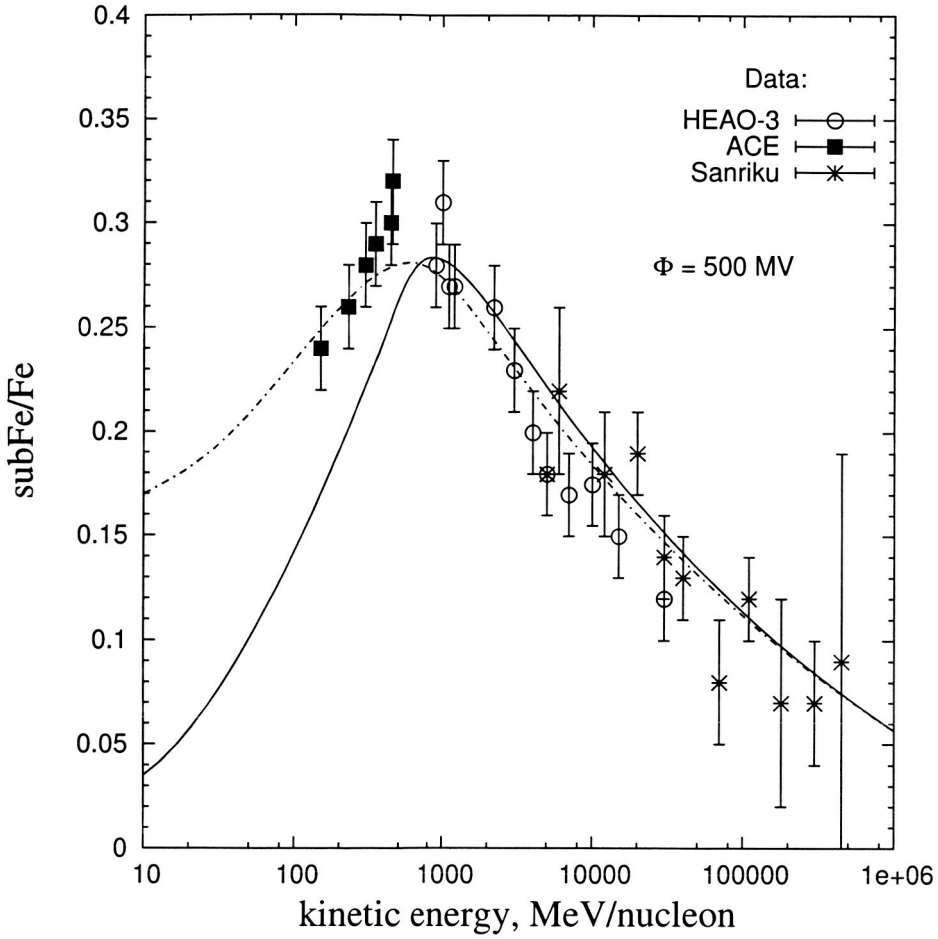

Fig. 3.— subFe/Fe ratio calculated for $z_h = 4$ kpc and $dV/dz = 0$. Solid curve (lower) local interstellar medium, dashed-dotted curve (upper) modulated $\phi = 500$ MV.

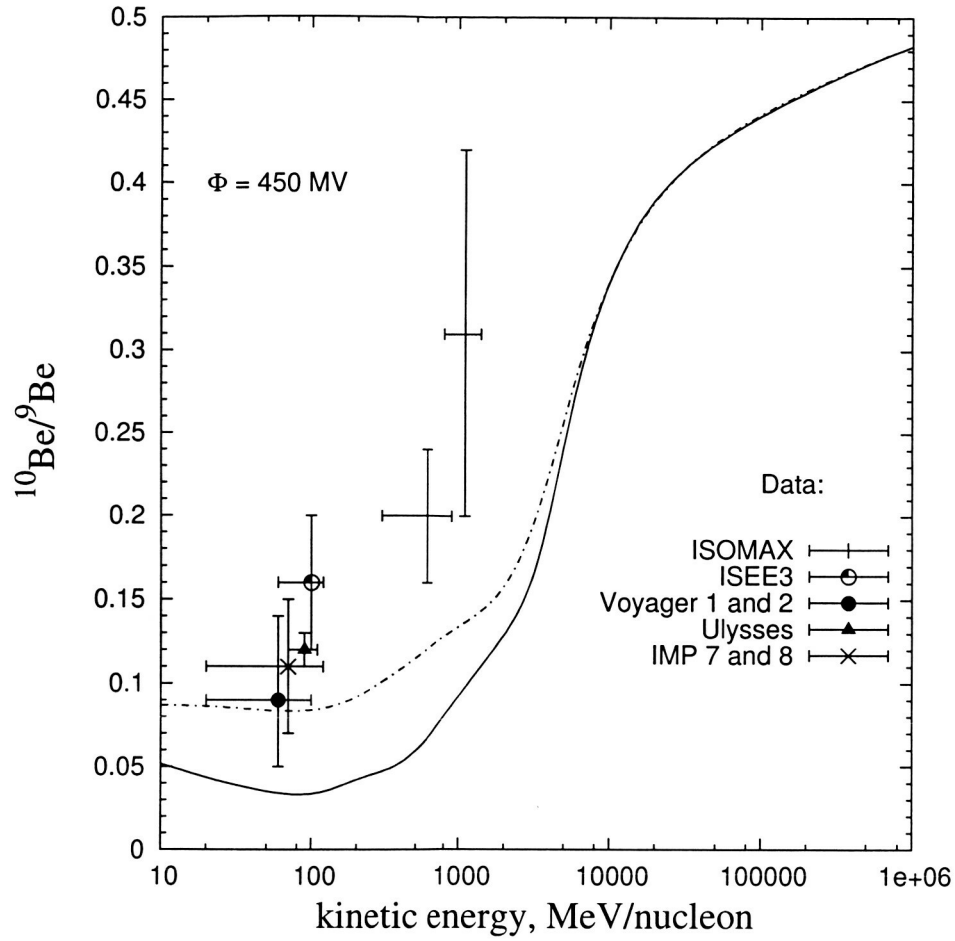

Fig. 4.— ^{10}Be/^{9}Be ratio calculated for $z_h = 4$ kpc and $dV/dz = 0$. Solid curve (lower) local interstellar medium, dashed-dotted curve (upper) modulated $\phi = 450$ MV.

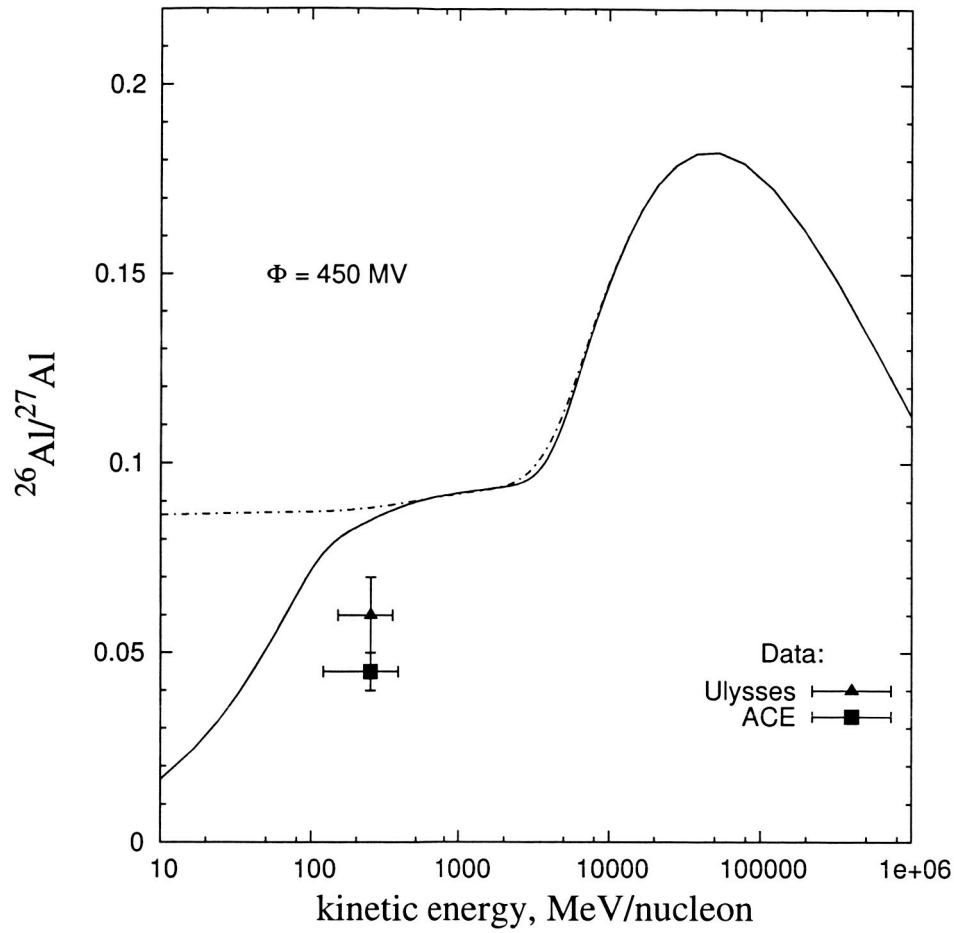

Fig. 5.— ^{26}Al/^{27}Al ratio calculated for $z_h = 4$ kpc and $dV/dz = 0$. Solid curve (lower) local interstellar medium, dashed-dotted curve (upper) modulated $\phi = 450$ MV.

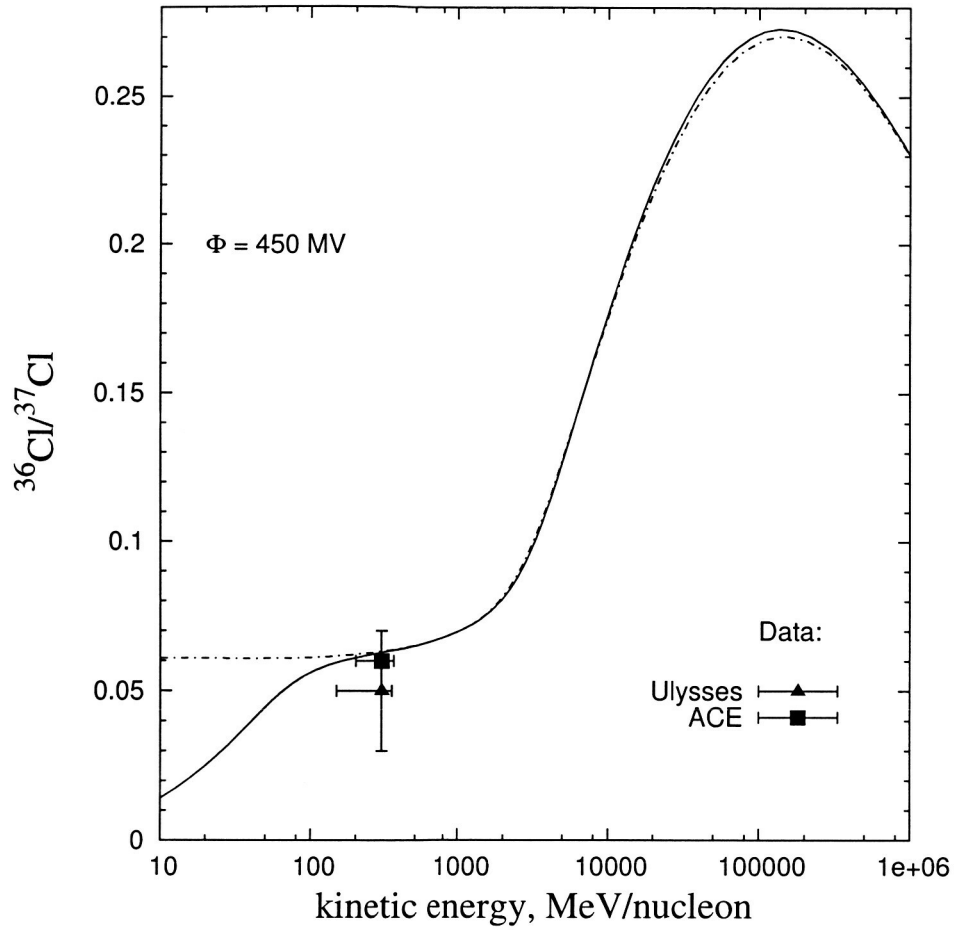

Fig. 6.— $^{36}Cl/^{37}Cl$ ratio calculated for $z_h = 4$ kpc and $dV/dz = 0$. Solid curve (lower) local interstellar medium, dashed-dotted curve (upper) modulated $\phi = 450$ MV.

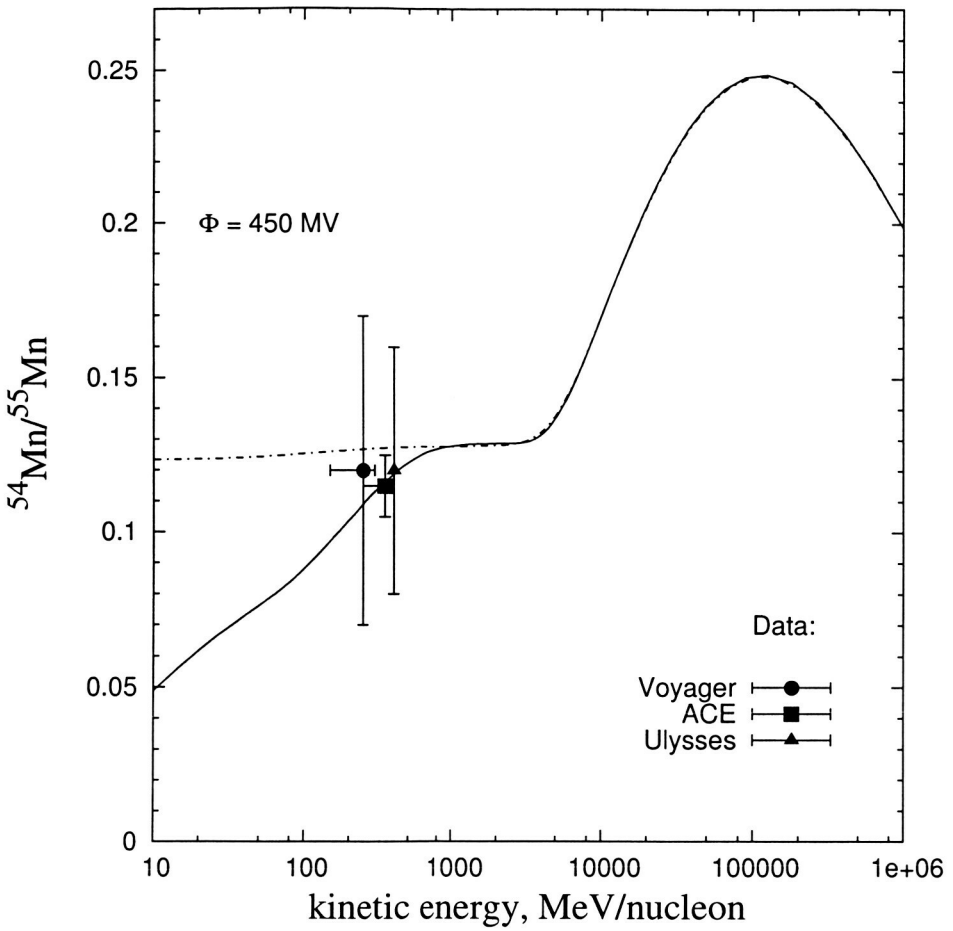

Fig. 7.— ^{54}Mn/^{55}Mn ratio calculated for $z_h = 4$ kpc and $dV/dz = 0$. Solid curve (lower) local interstellar medium, dashed-doted curve (upper) modulated $\phi = 450$ MV.

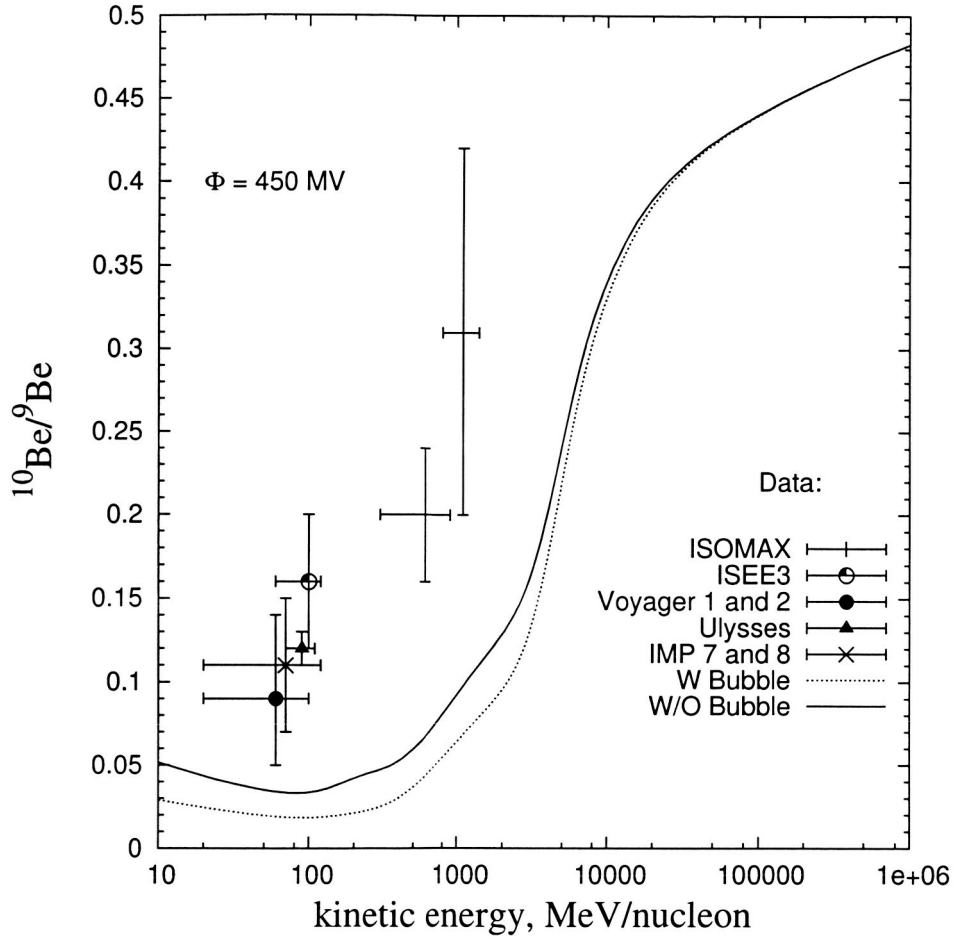

Fig. 8.— The effect of the low-density Local Bubble surrounding the solar system with radius of 200 pc and average density of 0.06 particles cm-3 on the ^{10}Be/^{9}Be ratio.

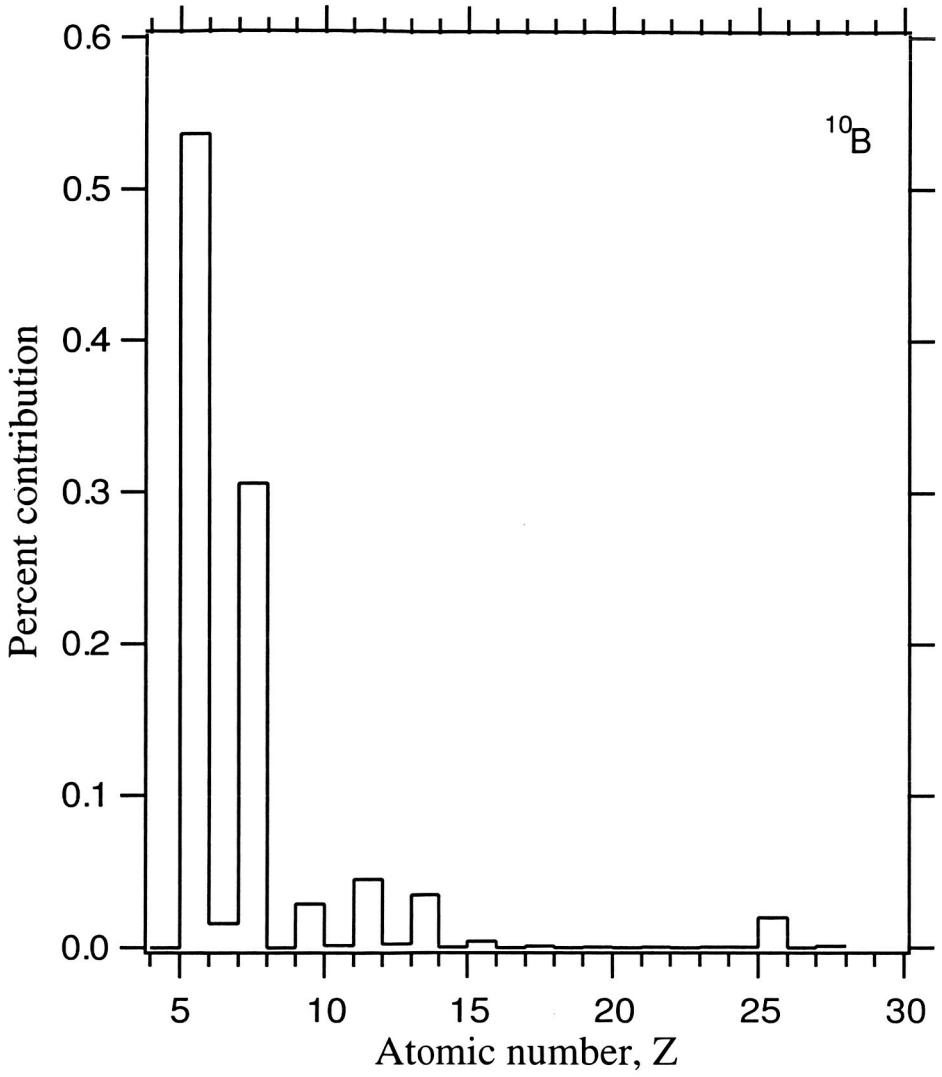

Fig. 9.— Elements percent contribution to the production of ^{10}B at 1 GeV/nucleon.

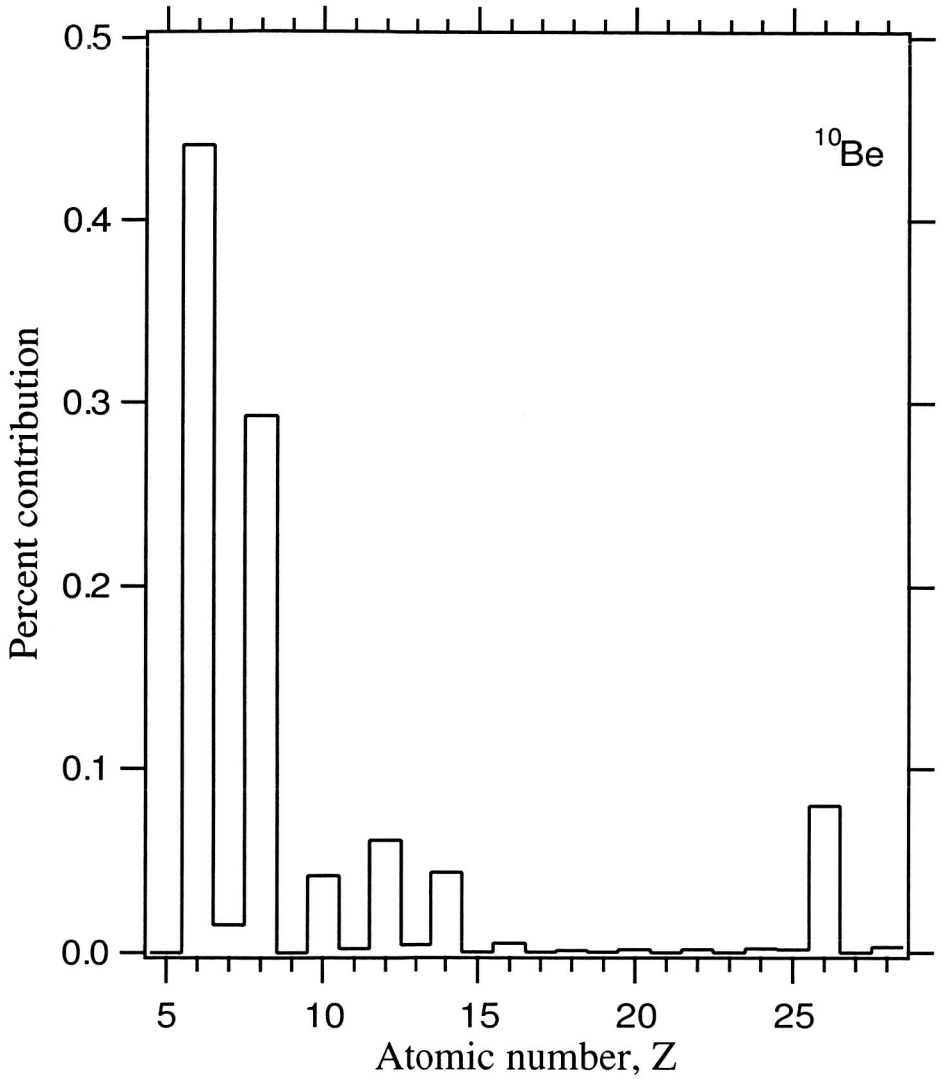

Fig. 10.— Elements percent contribution to the production of ^{10}Be at 1 GeV/nucleon.

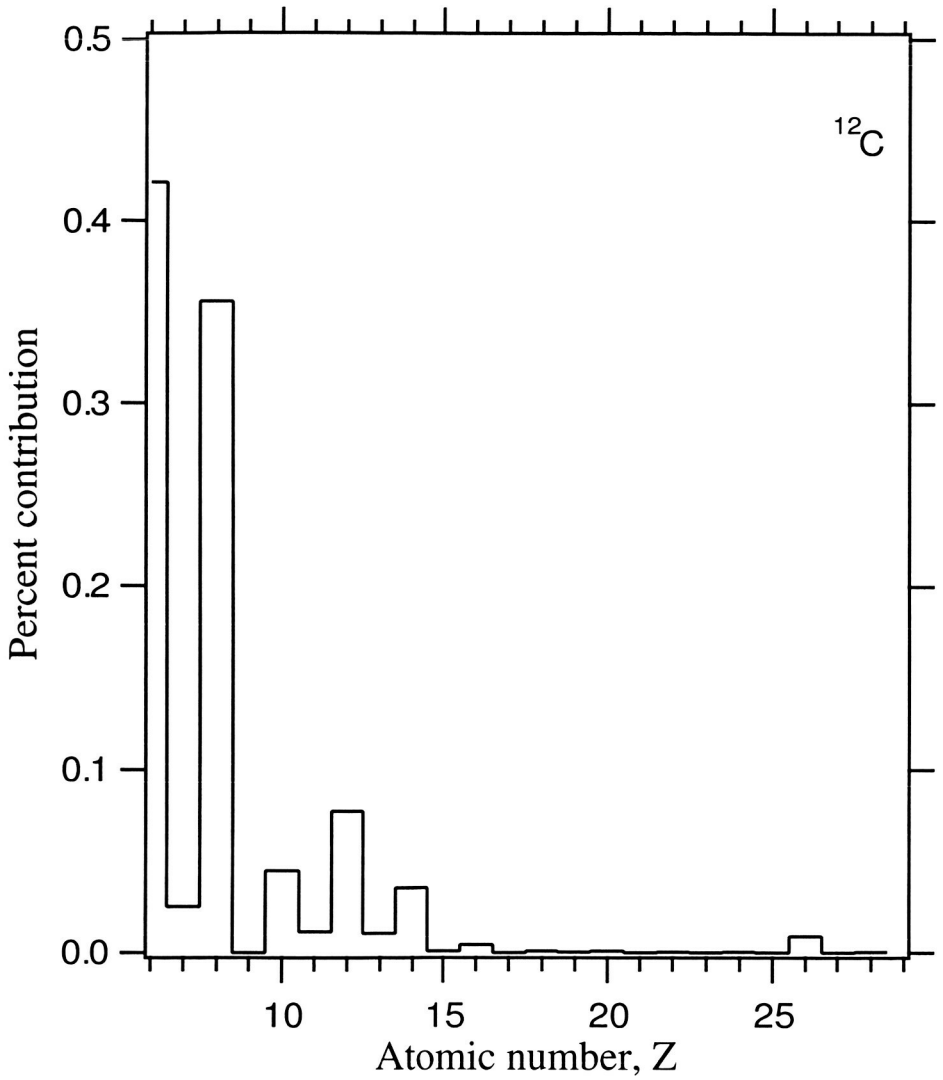

Fig. 11.— Elements percent contribution to the production of ^{12}C at 1 GeV/nucleon.

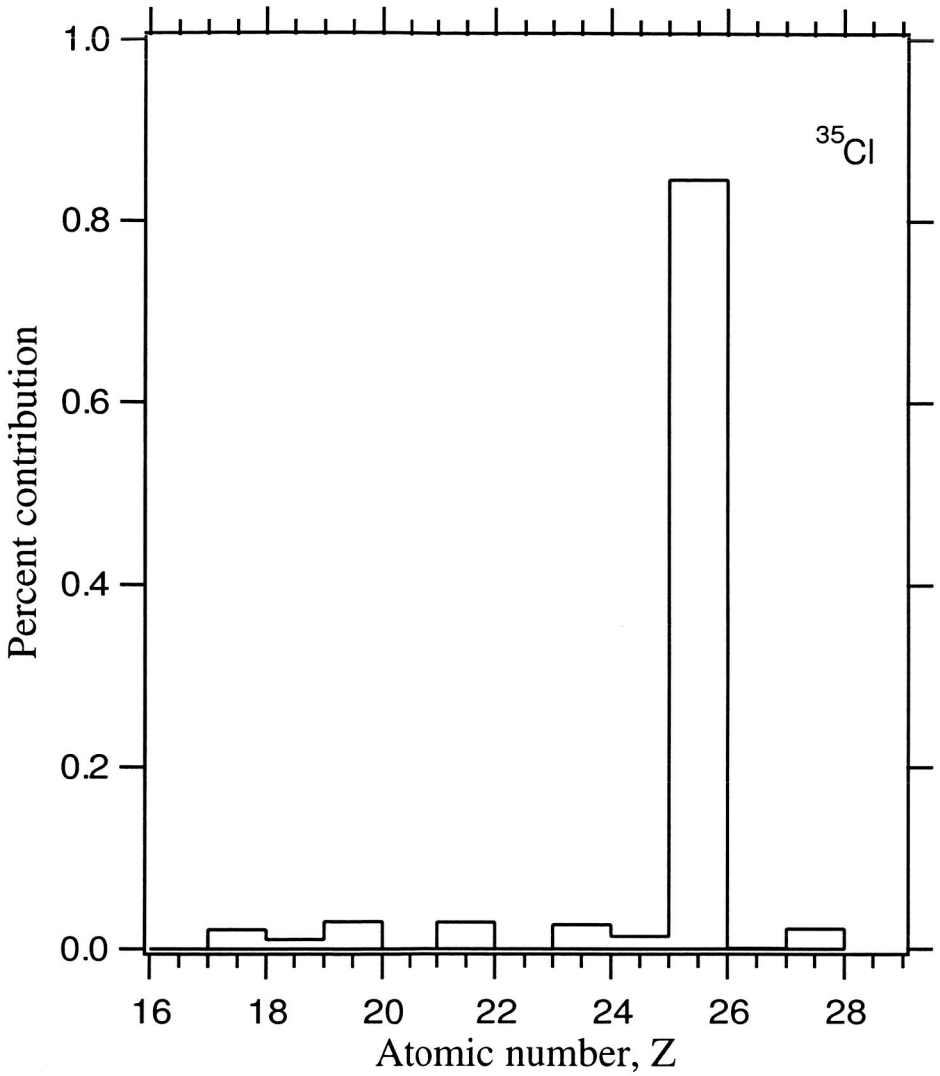

Fig. 12.— Elements percent contribution to the production of ^{35}Cl at 1 GeV/nucleon.

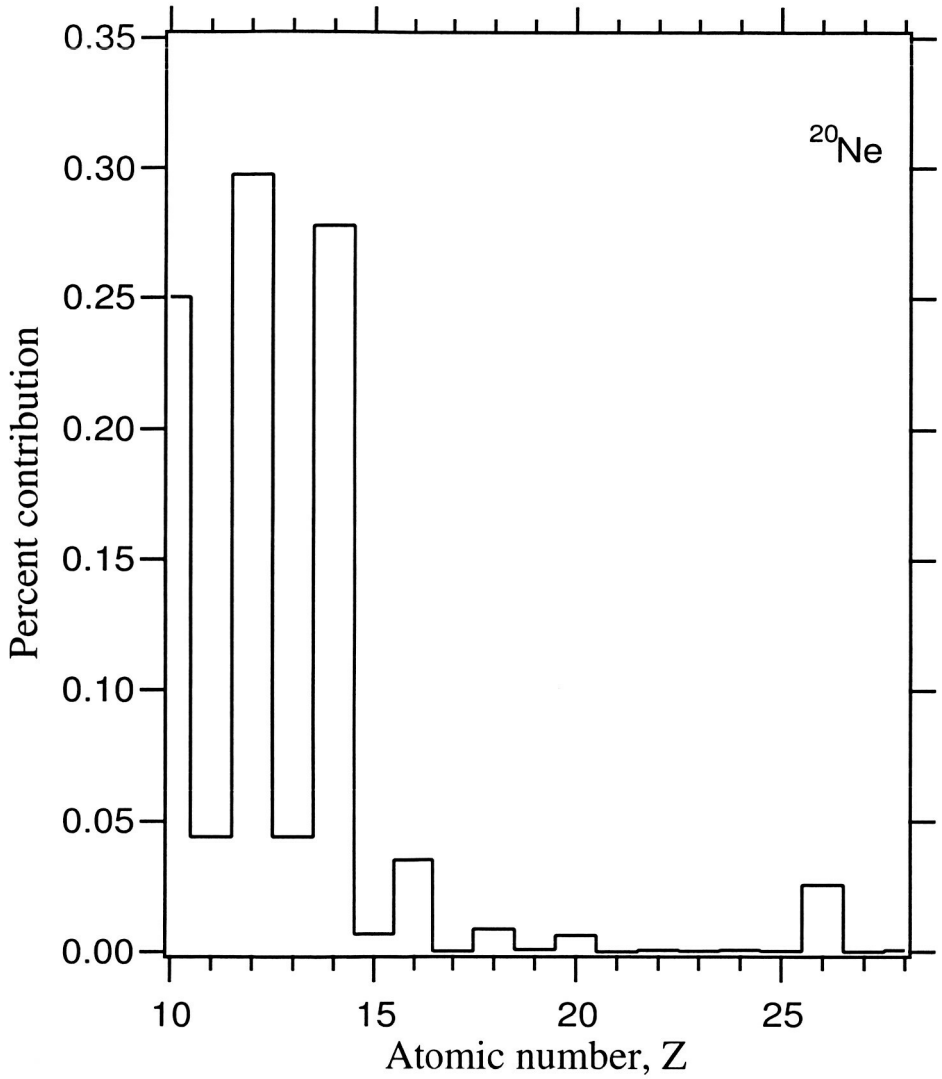

Fig. 13.— Elements percent contribution to the production of ^{20}Ne at 1 GeV/nucleon.

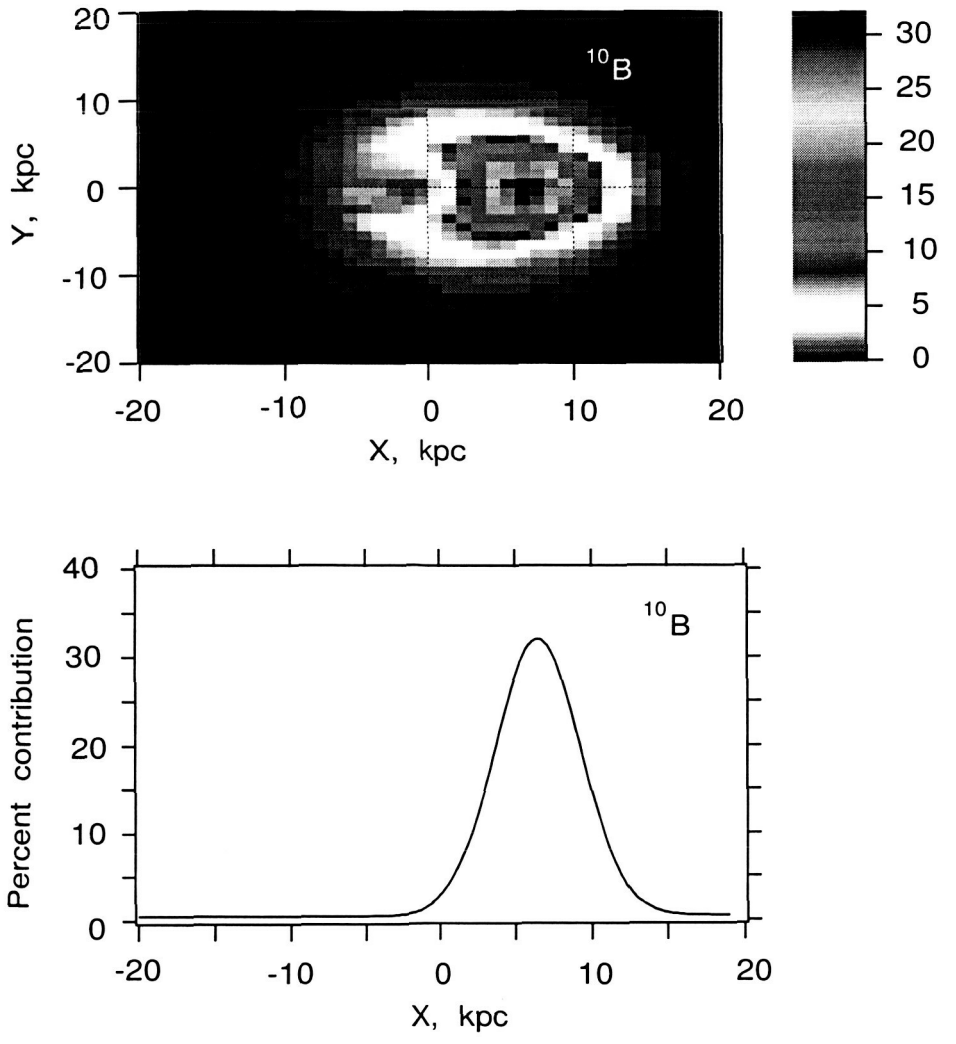

Fig. 14.— Upper plot: Contribution of various locations around the galaxy to the production of ^{10}B sources; model W/O Local Bubble; Energy = 1 GeV/nucleon and no modulation. Lower plot: ^{10}B Abundance normalized to (Carbon = 100) at Y = 0 and runs from -20 to 20 kpc. The solar system is located at X = 8.5 kpc, Y = 0 kpc and Z = 0 kpc; Curves are normalized to (Carbon = 100) at 1 GeV/nucleon.

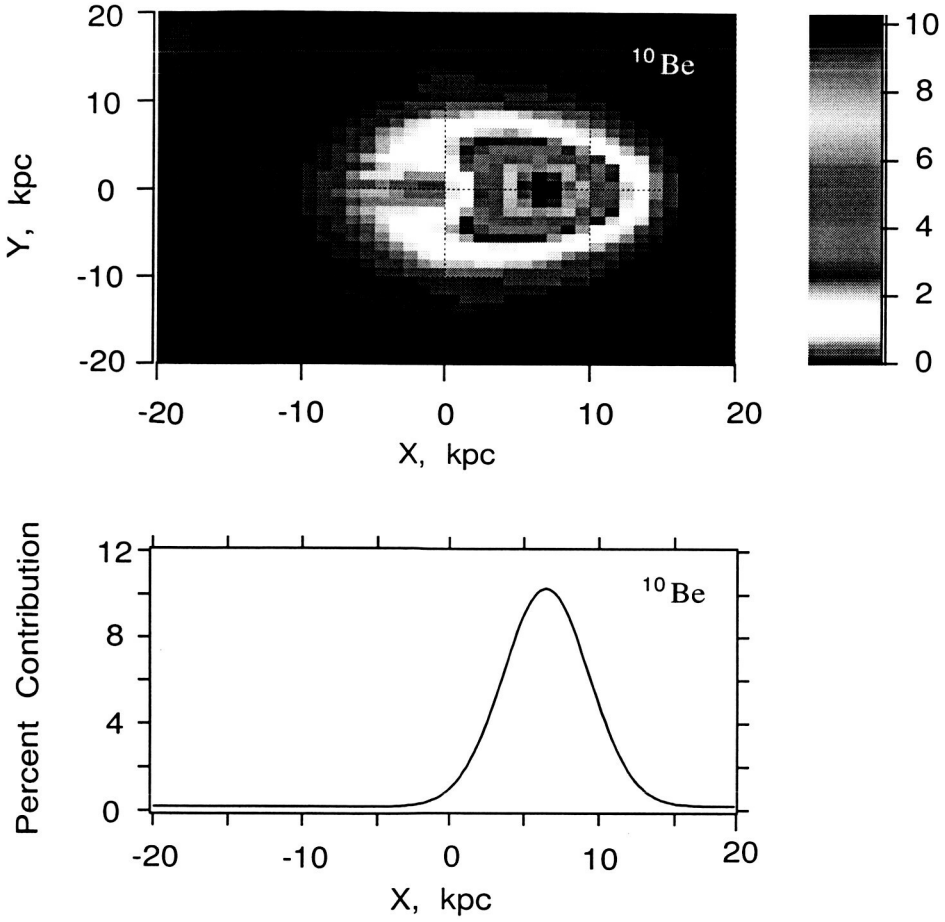

Fig. 15.— Upper plot: Contribution of various locations around the galaxy to the production of ^{10}Be sources; model W/O Local Bubble; Energy = 1 GeV/nucleon and no modulation. Lower plot: ^{10}Be Abundance normalized to (Carbon = 100) at Y = 0 and runs from -20 to 20 kpc. The solar system is located at X = 8.5 kpc, Y = 0 kpc and Z = 0 kpc; Curves are normalized to (Carbon = 100) at 1 GeV/nucleon.

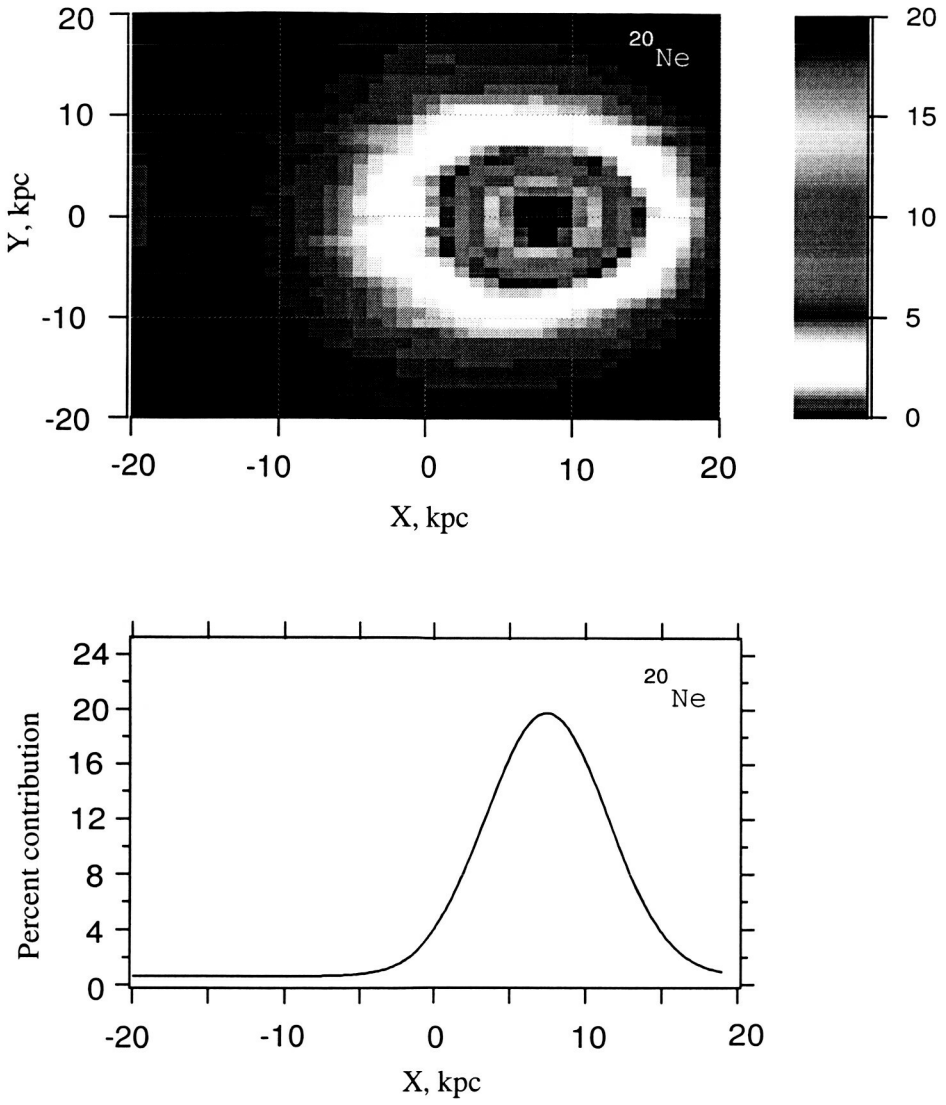

Fig. 16.— Upper plot: Contribution of various locations around the galaxy to the production of ^{20}Ne sources; model W/O Local Bubble; Energy = 1 GeV/nucleon and no modulation. Lower plot: ^{20}Ne Abundance normalized to (Carbon = 100) at Y = 0 and runs from -20 to 20 kpc. The solar system is located at X = 8.5 kpc, Y = 0 kpc and Z = 0 kpc; Curves are normalized to (Carbon = 100) at 1 GeV/nucleon.

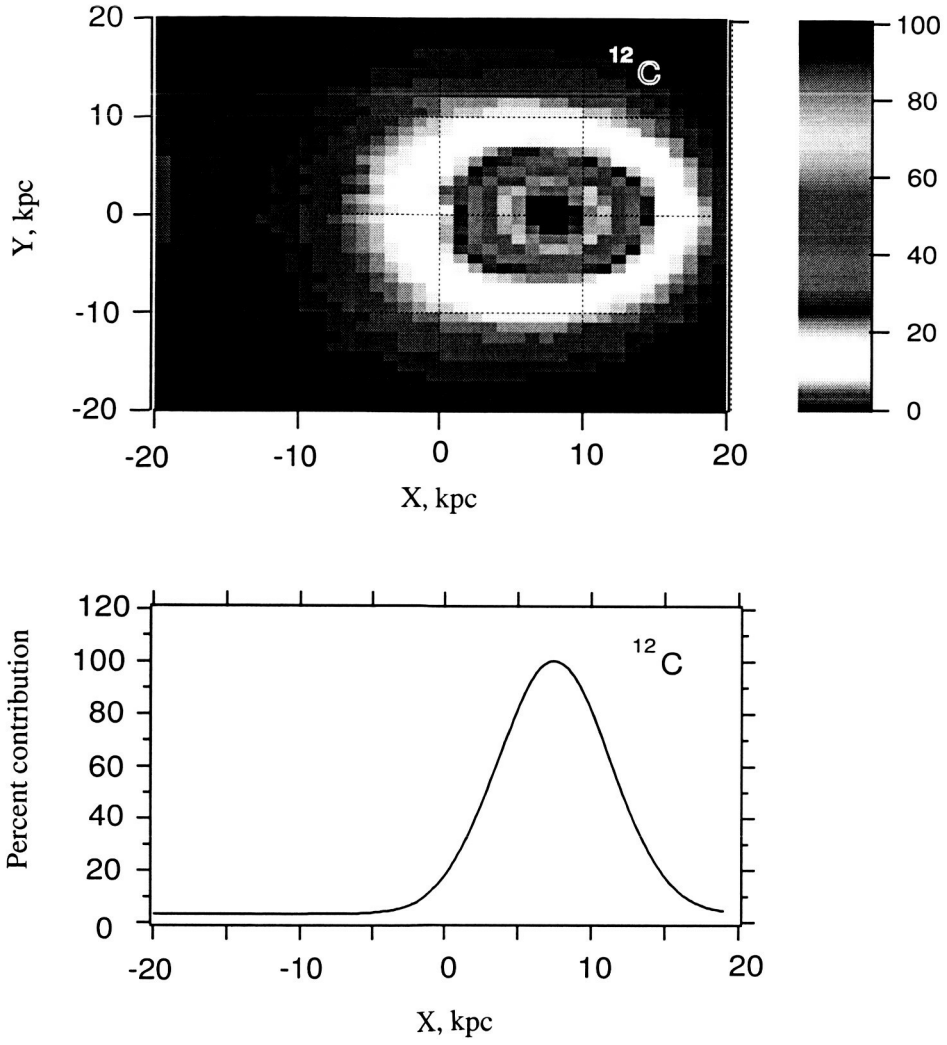

Fig. 17.— Upper plot: percent Contribution of various locations around the galaxy to the production of ^{12}C; model W/O Local Bubble; Energy = 1 GeV/nucleon and no modulation. Lower plot: ^{12}C percent contribution at Y = 0 and runs from -20 to 20 kpc. The solar system is located at X = 8.5 kpc, Y = 0 kpc and Z = 0 kpc at 1 GeV/nucleon.